Antibodies

DOI: 10.1002/ange.200503328

Epitope Mapping of the Protective Antigen of *B. Anthracis* by Using Nanoclusters Presenting Conformational Peptide Epitopes**

Aren E. Gerdon, David W. Wright, and David E. Cliffel**

Epitope mapping is the process of determining the major antibody binding sites on an antigen and can provide valuable information to one who is attempting to understand an antigen's mode of action or produce an antiviral vaccine. There are established techniques for the mapping of an antigen, including Western Blot analysis, X-ray crystallography, NMR spectroscopy, antibody competition assays, site-specific mutagenesis, and flow cytometry.[1–4] Each of these techniques have advantages and disadvantages and tend to excel in one particular aspect of epitope mapping. Many of these experiments place emphasis on distinguishing between discontinuous epitopes (contact points are far apart in amino acid sequence but proximal through space) and continuous epitopes (sequential amino acid sequence).[5] Unfortunately, these techniques often ignore conformations intrinsic to sequential epitopes. Consequently, many mapping techniques lack the ability to maintain the secondary structure (local conformation) of antigens or ignore it entirely despite the tremendous impact secondary structure can have on the location of contact points and, ultimately, antigenicity. Peptide epitopes are another tool for mapping sequential epitopes and have traditionally been used in the creation of synthetic peptide libraries and in phage display methods.[1,6] Again, these methods preclude the study of secondary structure, although they offer the best potential to incorporate conformation.

Research herein has established a method for the study of secondary-structure conformational effects on monoclonal-antibody binding to peptide epitopes. According to this method, we have effectively mapped monoclonal antiprotective antigen (anti-PA) antibodies to a protein conformational-loop region through the assembly of a conformational-loop epitope on a nanoparticle. Previously, cyclization of peptides has approximated loop structures with limited success,[7] but the development and presentation of a peptide that reconstitutes a physiological conformation is paramount (Figure 1).

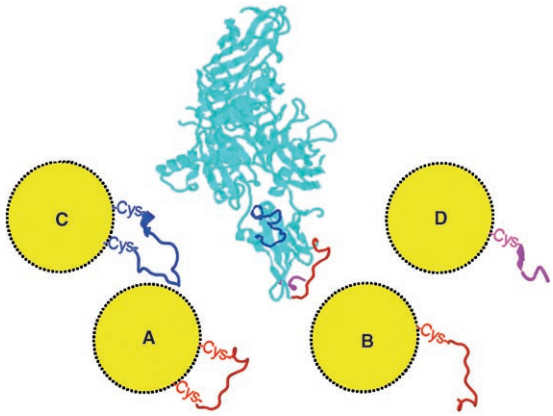

Figure 1. X-ray crystal structure of the protective antigen of *B. anthracis* (middle) and illustrations of PA mimics highlighting the conformational and linear epitopes. Three known epitopes are highlighted in the crystal structure: amino acids 680–692 (red), 703–722 (blue), 730–735 (magenta).[3,4,8–11] Composition of antigen mimics are as follows: A) PA680B–MPC = $Au_{807}Tiop_{290}Pep_4$; B) PA680M–MPC = $Au_{807}Tiop_{294}Pep_4$; C) PA703B–MPC = $Au_{807}Tiop_{282}Pep_8$; D) PA730M–MPC = $Au_{807}Tiop_{288}Pep_{10}$.

We have emphasized loop structures for several reasons: 1) surface accessible loops are abundant in many protein antigens, 2) previous epitope-mapping experiments have revealed loops as common antibody binding sites,[1,5,8,9] 3) loops are more amenable to nanocluster recapitulation when compared with other types of secondary structures. Surface accessible loops also lack steric interference and are highly solvated.

An example of a loop-rich protein is the protective antigen (PA) of *B. anthracis*, which is one of three protein precursors to the anthrax toxin. Edema factor (EF) and lethal factor (LF) depend on PA for membrane transport and activation and as a result, the binding of PA to the cell membrane is crucial for toxicity. PA has been a target for immunological studies that have shown that levels of anti-PA antibodies correlate well with an immunity to anthrax. Further examination has identified two loops and the C terminus as cell-receptor binding sites, and therefore, possible sites for toxin neutralization by immunoglobulin G (Figure 1).[2,4,8–11] Recent studies[3] with denatured and non-denatured PA confirm the necessity of conformation in loop structures and also suggest the presence of a linear epitope, such as the C terminus. The identification of these loops, and the high priority that anthrax has received owing to its potential as a bioterrorism agent make PA an excellent model for the design of complex, conformational nanostructures that mimic an antigen and have the ability to interface with biological systems.

Research at this interface between biology and nanomaterials is of recent interest and has produced a number of

[*] A. E. Gerdon, Dr. D. W. Wright, Dr. D. E. Cliffel
Department of Chemistry
Vanderbilt University
Station B 351822
Nashville, TN 37235 (USA)
Fax: (+1) 615-343-1234
E-mail: david.wright@vanderbilt.edu
d.cliffel@vanderbilt.edu

[**] This research was funded in part by a Vanderbilt Institute of Chemical Biology fellowship (A.E. Gerdon), the Chemical Biology Interface training grant (AE Gerdon, T32 GM065086), and the Vanderbilt Institute of Nanoscale Science and Engineering (A.E. Gerdon). DWW acknowledges support from the SouthEast Regional Center of Excellence for Biodefense (NIH U54 AI57157-03).

Supporting information for this article is available on the WWW under http://www.angewandte.org or from the author.

exciting and successful examples of well-defined interfaces.[12,13] Progress towards specifically interfacing immunology with nanoparticles is highlighted by an important approach that made use of a peptide epitope that is known to bind monoclonal antibodies associated with the human malarial parasite, *P. falciparum*. This was the first example of antigen-encapsulated nanoclusters that assemble with antibodies through the antibody/epitope interface.[14] A more-recent example used glutathione-encapsulated nanoclusters and polyclonal antiglutathione antibodies. This approach confirmed the ability to assemble single-component monolayer nanoclusters with antibodies and provided an analytical technique for rigorous evaluation of interface assembly by using the quartz crystal microbalance.[15]

More-complex nanostructures, which specifically present peptide epitopes in a dual-component monolayer, require scaffold properties that are common to monolayer-protected clusters (MPCs). MPCs capped with a tiopronin ligand are water soluble, their average diameter (ranging from approximately 2 to 5 nm) is on the order of small proteins,[15–17] they are easily characterized by conventional techniques and have convenient optical and electronic properties,[18] the ligand (a thiolated derivative of glycine) is relevant to biological systems and provides the cluster with an overall negative charge.[17] Further functionalization of the cluster through ligand coupling or place-exchange reactions is facile and has been well studied.[19]

Presentation of peptide epitopes on the surface of Tiop–MPC can provide functionality and has been carried out through well-characterized place-exchange reactions.[19,20] This provides the ease of functionalization of MPCs, which makes them attractive as protein mimics and as functional nanostructures. An important feature of place-exchange reactions and the presentation of conformational peptide epitopes is the idea that fast-exchange sites are not static. Evidence for this has come from the exchange of several different ligands onto the same MPC[21,22] and from an inability to completely remove ligands that had been previously exchanged onto a cluster.[19,22] A significant implication of these results is the ability of thiolate to migrate across the monolayer of an MPC. This migration might allow for the faithful reconstitution of a peptide epitope if the two ends of a bidentate ligand are able to move and position themselves at a distance similar to that in their physiological conformation.

The peptide epitopes, shown in Table 1, were synthesized for presentation on MPCs. Cystein (cys) residues were added at the N and/or C terminus to promote bidentate or monodentate exchange and alanine (ala) residues were similarly added for a lack of reactivity or presentation. Concurrently, water-soluble, nanometer-sized, monolayer-protected clusters were synthesized with tiopronin, a glycine derivative, as the passivating ligand as was reported previously.[15,17] Careful characterization allowed for the calculation of a diameter of 3.5 ± 1.0 nm and an estimated composition of $Au_{807}Tiop_{298}$ (207 kDa; see the Supporting Information). This size is close to the estimated optimal MPC size for the bidentate attachment of peptide PA680B (see the Supporting Information). The epitope and MPC scaffold were then brought together through place-exchange reactions to produce functional nanostructures.[19,22] Following each exchange, the extent of presentation was determined by ^{1}H NMR spectroscopy (see the Supporting Information). A cartoon schematic and final composition of antigen mimics can be seen in Figure 1.

Table 1: Amino acid sequences for peptides used in antigen mimic design.[a]

Peptide	Sequence	MW [Da]	Reference
PA680B	**C** KYNDK LPLYI SNP **C**	1771	[3, 4, 8–11]
PA680M	KYNDK LPLYI SNP **C**	1668	[3, 4, 8–11]
PA680A	**AA** KYNDK LPLYI SNP **A**	1778	[3, 4, 8–11]
PA703B	**C** KENTI INPSE NGDTS TNGIK **C**	2339	[8–11]
PA730M	**C** KGYEI G	769	[4]

[a] Highlighted cys (**C**) and ala (**A**) were not part of the epitope but added for functionalization and immobilization purposes.

The faithful reconstruction of epitope loops in a physiologically relevant conformation is predicated based on the ability to assemble loop peptides in a bidentate fashion. A linear epitope, such as the C terminus of PA (PA730M), can easily be attached to the MPC in a monodentate fashion that affords the peptide a good chance of maintaining its correct conformation. On the other hand, peptide epitopes from flexible loop regions of proteins cannot undergo monodentate attachment and be expected to adopt the correct conformation. Immobilization of both ends of the peptide in a bidentate, bivalent model restrains the peptide and promotes a conformation comparable with its native form. This is not an attempt to "fold" the peptide, rather an attempt at placing the peptide in an environment similar to that of the intact protein.

One challenge was in the characterization of the mode of attachment. The diversity of particle size can affect loop attachment and create a large combinatorial set of epitope conformations. Techniques such as CD and two-dimensional NMR spectroscopy have been successful in the evaluation of peptide conformation. However, low concentration of peptides on the surface of the MPC, cluster absorbance, and characteristically broad NMR peaks limit the applicability to this study. Instead, the mode of peptide attachment to the nanocluster was probed with a free-thiol labeling molecule, Ellman's Reagent (ER).[23] The reaction of ER with free peptide PA680M produced a characteristic yellow color and, after purification, showed thiol derivatization in ^{1}H NMR and MALDI-MS spectra. Conversely, the reaction of ER with PA680B–nanocluster complex did not show any indication of derivatization (see the Supporting Information). Labeling experiments with ER have supported bidentate attachment through the indication of a lack of free, unattached thiol in an MPC solution (see the Supporting Information) but provide no information on conformation.

A further test of epitope conformation showed a difference in antibody binding between a linear and conformational antigen mimic. As a result, the development of a sensitive, selective, quantitative assay that allowed for 3D-nanocluster substrates, multilayer adsorptions, and nonrigid biological recognition was required. The quartz-crystal microbalance (QCM) has recently been demonstrated to be well suited for this type of assay.[15] It has been used in the study of a variety of biological and nonbiological systems[15,24] and has numer-

ous benefits over other techniques that compete for the study of nanoscale assembly.[13] A sensitive and selective immunosensor that involves a piezoelectric quartz crystal with a gold electrode and sequential layering of polyelectrolyte,[25,26] MPC, and blocking with bovine serum albumin (BSA), leads to the immobilization of antigen mimics and thus provides a foundation for antibody screening. The results of representative adsorption and average binding of polyelectrolyte (0–30 min), MPC (30–60 min), and BSA (80–100 min) can be seen in Figure 2 and Table 2, respectively (see also the Supporting Information). MPC antigen mimics bound to the sensor to varying degrees as a result of differences in peptide presentation and ionic charge. Although this might affect the density of the peptide available for antibody binding, it will not affect the affinity (K_a) of the antibody/epitope interaction.[20] Binding studies involved seven mouse monoclonal anti-PA antibodies obtained from Biodesign International. These antibodies were known to bind both the full-sized PA (83 kDa) and the furin-cleaved PA (63 kDa) (according to Western Blot) but had not been tested for their ability to neutralize the toxin.[27] To map the antibodies to different conformational and linear regions of the antigen, the antibodies were screened at constant concentration against the four PA mimics. At a relatively low concentration of antibody (124 nM), screening experiments provided qualitative information on the recognition or lack of recognition and as such, guided further studies (Table 2). The results of the screening experiments suggest cross reactivity for several antibodies, and antibody 110 was identified as being potentially selective for the conformational epitope spanning amino acids 680–692.

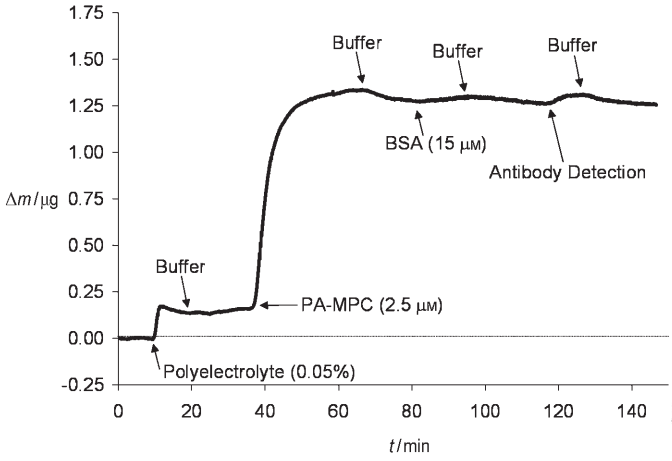

Figure 2. Representative polyelectrolyte, PA680B–MPC, BSA, and antibody 110 binding in phosphate buffer solution.

Table 2: Results of immunosensor assembly (μg) and for screening monoclonal anti-PA antibodies (124 nM) against four antigen mimics (in ng).[a]

	PA680B	PA680M	PA703B	PA730M
Ave PolyE	0.16 ± 0.03	0.16 ± 0.03	0.16 ± 0.03	0.16 ± 0.03
Ave MPC	1.12 ± 0.06	0.80 ± 0.07	0.73 ± 0.06	0.68 ± 0.07
Ave BSA	0.06 ± 0.05	0.13 ± 0.05	0.14 ± 0.02	0.21 ± 0.02
mAb 110	20	10	0	0
mAb 201	15	0	10	14
mAb 301	0	10	0	0
mAb 410	10	0	10	16
mAb 501	10	10	0	11
mAb 601	10	10	0	10
mAb 613	13	0	10	10

[a] Screening was completed by using QCM and all values represent changes in mass. Data suggest antibody 110 as having strong and specific interaction with PA680B–MPC.

This antibody was studied in more detail through variation of the antibody concentration and the ionic strength of buffer solutions. Seven experiments for each of the two antigen mimics (PA680B–MPC and PA680M–MPC), differing only in mode of peptide attachment (bidentate versus monodenate), showed saturation of the immunosensor. The four-highest concentrations for each mimic were fit to a logarithmic curve (Figure 3). Equilibrium association constants (K_a) were determined for each mimic by fitting the four-highest concentrations to a Langmuir adsorption isotherm (Table 3).[13,15,28] PA680B–MPC had a K_a of $(5.9 \pm 0.7) \times 10^6\,M^{-1}$, which falls within a general range for immunoaffinity

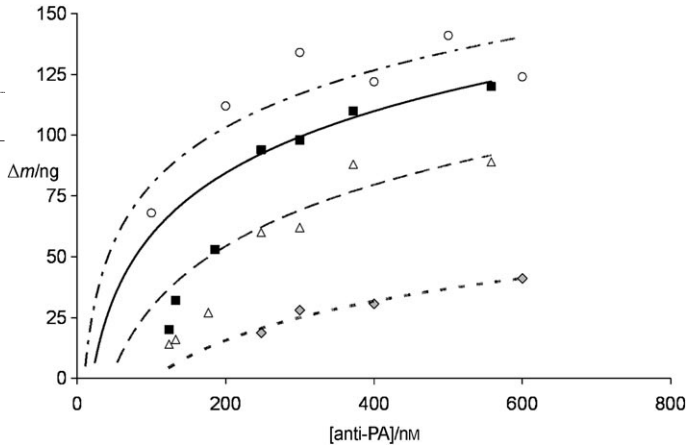

Figure 3. Plot of Δm against [anti-PA] for PA protein antigen (○) with logarithmic fit to six doses (– – –), PA680B–MPC (■) with logarithmic fit to four doses of high concentration (——), MPC–PA680M (△) with logarithmic fit to four doses of high concentration (– – –), and PA680B–MPC (◇) in PBS with logarithmic fit (-----) showing saturation of the immunosensor in all cases.

Table 3: Results from equilibrium calculations for two antigen mimics and the Protective Antigen protein.[a]

Antigen	[NaCl] mM	Equilibrium Constants K_a [$\times 10^6\,M^{-1}$]
MPC-PA680B	0	5.9 ± 0.7
	0	4.0 ± 0.8[b]
	150	2 ± 1
MPC-PA680M	0	2.6 ± 0.9
	150	–[c]
Protective Antigen	0	12 ± 6

[a] Experiments were conducted in phosphate buffer solution (no added NaCl) or in phosphate-buffered saline solution (150 mM NaCl). [b] Equilibrium constant calculated from kinetic constants, where $K_a = k_f/k_r$. [c] Unable to calculate owing to a lack of binding.

of 10^6–$10^{10}\,\text{M}^{-1}$ [29] and shows an increased affinity over a previously reported glutathione-presenting nanocluster with polyclonal antibody ($K_a = 3.6 \times 10^5\,\text{M}^{-1}$).[15] Antibody 110 had a decreased affinity for the linear epitope-presenting nanocluster (PA680M–MPC, $K_a = (2.6 \pm 0.9) \times 10^6\,\text{M}^{-1}$), which suggests a real difference between peptide epitopes of identical primary structure but different secondary structure.

These results were validated through control experiments by using Tiop–MPC and buffer solutions of increasing ionic strength (Figure 4). Salt gradients are typically used in affinity

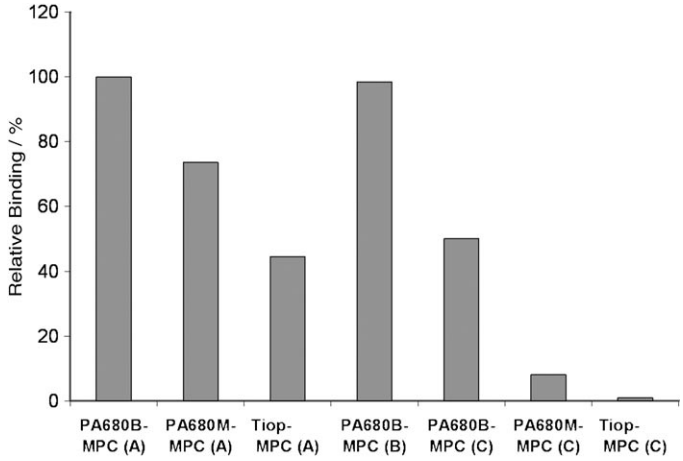

Figure 4. Relative binding percent for antibody 110 (300 nM) to seven different nanocluster systems, normalized to density of nanocluster displayed on immunosensor surface. All samples were run in phosphate buffer solution (50 mM) with varying concentrations of NaCl (A = 0 mM, B = 50 mM, C = 150 mM).

chromatography and are known to decrease weak interactions.[30] In initial studies, the background antibody binding to Tiop–MPC and PA680M–MPC in phosphate buffer solution (50 mM) was relatively high. The addition of NaCl (150 mM) decreased the weak, nonspecific adsorption seen in Tiop–MPC and PA680M–MPC but had a significantly lower effect on PA680B–MPC. Furthermore, a decreased concentration of NaCl (50 mM) had essentially no effect on antibody binding to PA680B–MPC. This allowed for the study of concentration dependence of antibody 110 binding to PA680B–MPC in high-ionic-strength buffer solution. The association constant ($K_a = (2 \pm 1) \times 10^6\,\text{M}^{-1}$) was only slightly less than that calculated in low-ionic-strength buffer solution (Figure 3) and confirmed strong recognition and limited nonspecific adsorption.

Kinetic information calculated for PA680B–MPC ($k_f = (9 \pm 2) \times 10^3\,\text{M}^{-1}\,\text{s}^{-1}$ and $k_r = (2.3 \pm 0.5) \times 10^{-3}\,\text{s}^{-1}$) from the time-dependent binding curves supports the equilibrium data and the immunorecognition of antibodies to conformational mimics. The equilibrium adsorption constant, K_a, is equal to the ratio of k_f/k_r and was calculated to be $(4.0 \pm 0.8) \times 10^6\,\text{M}^{-1}$, which correlates well with the K_a found in the previous method (Figure 3). Kinetic constants relate to the kinetics of polyclonal antibody binding to glutathione–MPC, with $k_f = 5.4 \times 10^1\,\text{M}^{-1}\,\text{s}^{-1}$ and $k_r = 1.5 \times 10^{-4}\,\text{s}^{-1}$.[15] It is reasonable that this forward rate constant is less than that for monoclonal anti-PA antibody owing to the heterogeneity of the polyclonal anti-glutathione sample. The binding kinetics for the snake neurotoxin, α-bungarotoxin, to synthetic peptide mimotopes have been reported[31] with k_f in the range of 10^1–$10^4\,\text{M}^{-1}\,\text{s}^{-1}$ and k_r in the range of 10^{-3}–$10^{-4}\,\text{s}^{-1}$. The kinetic rate constants for antibody 110 binding to PA680B–MPC also fall within these ranges.

Antibody binding to an intact protein antigen was studied for comparison with the antigen mimics. The antibody was shown to specifically bind the protein with a K_a value slightly larger than that calculated for the nanocluster antigen mimic (Figure 3, Table 3). The antibody did display high background adsorption to BSA in phosphate buffer solution (50 mM), but decreased in high-ionic-strength buffer solution, whereas antibody binding to PA was only slightly affected by an increase in ionic strength. Furthermore, anti-hemagglutinin (HA) antibody, which is not specific for PA, showed no binding to PA in low-ionic-strength buffer solution. The similarity between antigen and antigen-mimic K_a values points to the exceptional reconstitution of the conformational peptide epitope on the surface of the nanocluster.

The sum of these results suggests several things about the efficacy of these complex antigen mimics. First, it is apparent that we are able to successfully assemble peptides on nanoclusters to produce functional, immunoreactive nanoscale components. Second, we are able to employ functionalized nanoclusters in the screening of available monoclonal antibodies and effectively map an antibody to a peptide epitope. Finally, we were able to differentiate between conformational and linear epitopes and map a monoclonal antibody accordingly. Antibody 110 has an apparent increased affinity ($> 2\times$) for the conformational antigen mimic over the linear antigen mimic and an even greater affinity difference when in isotonic ionic-strength buffer solutions. Control experiments confirmed the enhanced affinity and placed the antigen mimic in the same affinity range as the intact protein. These antibodies could be used in the selection and isolation of tight binding, conformationally relevant antigen mimics, therefore providing information which could guide future mimic assembly. The placement of artificial conformational epitopes on a nanoparticle framework represents a significant early advance in our ability to control immunomodulation at the nanoscale.

Received: September 19, 2005
Published online: December 15, 2005

Keywords: antibodies · biomimetic synthesis · biosensors · immunoassays · nanostructures

[1] G. E. Morris, in *Epitope Mapping Protocols, Vol. 66*, Humana Press, Totowa, NJ, **1996**, pp. 1–9.
[2] E. Santelli, L. A. Bankston, S. H. Leppla, R. C. Liddington, *Nature* **2004**, *430*, 905–908.
[3] M. A. Wild, H. Xin, T. Maruyama, M. J. Nolan, P. M. Calveley, J. D. Malone, M. R. Wallace, K. S. Bowdish, *Nat. Biotechnol.* **2003**, *21*, 1305–1306.
[4] D. S. Reed, J. Smoll, P. Gibbs, S. Little, *Cytometry* **2002**, *49*, 1–7.

[5] M. H. V. Van Regenmortel, *Philos. Trans. R. Soc. London Ser. B* **1989**, *323*, 451 – 466.
[6] S. R. Whaley, D. S. English, E. L. Hu, P. F. Barbara, A. M. Belcher, *Nature* **2000**, *405*, 665 – 668.
[7] S. Misumi, M. Endo, R. Mukai, K. Tachibana, M. Umeda, T. Honda, N. Takamune, S. Shoji, *J. Biol. Chem.* **2003**, *278*, 32335 – 32343.
[8] S. Leppla, J. Robbins, R. Schneerson, J. Shiloach, *J. Clin. Invest.* **2002**, *109*, 141 – 144.
[9] C. Petosa, R. J. Collier, K. R. Klimpel, S. H. Leppla, R. C. Liddington, *Nature* **1997**, *385*, 833 – 838.
[10] S. Little, J. P. Novak, J. R. Lowe, S. Leppla, Y. Singh, K. R. Klimpel, B. C. Lidgerding, A. Friedlander, *Microbiology* **1996**, *142*, 707 – 715.
[11] H. C. Flick-Smith, N. J. Walker, P. Gibson, H. Bullifent, S. Hayward, J. Miller, R. W. Titball, E. D. Williamson, *Infect. Immun.* **2002**, *70*, 1653 – 1656.
[12] C. M. Niemeyer, *Angew. Chem.* **2001**, *113*, 4254 – 4287; *Angew. Chem. Int. Ed.* **2001**, *40*, 4128 – 4158.
[13] A. E. Gerdon, D. W. Wright, D. E. Cliffel in *Characterization Tools for Nanosystems in Life Sciences* (Ed.: C. Kumar), Wiley-VCH, New York, **2005**, pp. 109 – 144.
[14] J. M. Slocik, J. T. Moore, D. W. Wright, *Nano Lett.* **2002**, *2*, 169 – 173.
[15] A. E. Gerdon, D. W. Wright, D. E. Cliffel, *Anal. Chem.* **2005**, *77*, 304 – 310.
[16] A. C. Templeton, S. Chen, S. M. Gross, R. W. Murray, *Langmuir* **1999**, *15*, 66 – 76.
[17] A. C. Templeton, D. E. Cliffel, R. W. Murray, *J. Am. Chem. Soc.* **1999**, *121*, 4845 – 4849.
[18] M. J. Hostetler, J. E. Wingate, C.-J. Zhong, J. E. Harris, R. W. Vachet, M. R. Clark, J. D. Londono, S. T. Green, J. J. Stokes, G. D. Wignall, G. L. Glish, M. D. Porter, N. D. Evans, R. W. Murray, *Langmuir* **1998**, *14*, 17 – 30.
[19] M. J. Hostetler, A. C. Templeton, R. W. Murray, *Langmuir* **1999**, *15*, 3782 – 3789.
[20] A. E. Gerdon, D. W. Wright, D. E. Cliffel, *Biomacromolecules* **2005**, *6*, 3419 – 3424.
[21] R. S. Ingram, M. J. Hostetler, R. W. Murray, *J. Am. Chem. Soc.* **1997**, *119*, 9175 – 9178.
[22] A. C. Templeton, M. J. Hostetler, E. K. Warmoth, S. Chen, C. M. Hartshorn, V. M. Krishnamurthy, M. D. E. Forbes, R. W. Murray, *J. Am. Chem. Soc.* **1998**, *120*, 4845 – 4849.
[23] Ellman's Reagent, http://www.piercenet.com/files/0311h4.pdf, **2004**.
[24] A. Janshoff, H. J. Galla, C. Steinem, *Angew. Chem.* **2000**, *112*, 4164 – 4195; *Angew. Chem. Int. Ed.* **2000**, *39*, 4004 – 4032.
[25] G. Decher, *Science* **1997**, *277*, 1232 – 1237.
[26] A. A. Mamedov, A. Belov, M. Giersig, N. N. Mamedova, N. A. Kotov, *J. Am. Chem. Soc.* **2001**, *123*, 7738 – 7739.
[27] Biodesign International, http://www.biodesign.com, **2004**.
[28] The rate of antibody adsorption is directly proportional to the bulk concentration of antibody (rate = k_f[antibody]). In the time frame of this experiment (10 min flow at 30 μL/min) high concentrations of antibody reached equilibrium, but low concentrations did not. For this reason, low concentrations did not give changes in mass that are consistent with equilibrium adsorption and were not used in calculations.
[29] D. L. Nelson, M. M. Cox, *Lehninger Principles of Biochemistry*, 3rd ed., Worth Publishers, New York, **2000**.
[30] M. A. J. Godfrey in *Affinity Separations* (Ed.: P. Matejtschuk), IRL, Oxford, **1997**, pp. 141 – 193.
[31] L. Bracci, L. Lozzi, B. Lelli, A. Pini, P. Neri, *Biochemistry* **2001**, *40*, 6611 – 6619.

